Inorganic Chemistry

Article

pubs.acs.org/IC

Dynamics of Zn^{II} Binding as a Key Feature in the Formation of Amyloid Fibrils by Aβ11-28

Bruno Alies,[†,‡] Pier-Lorenzo Solari,[§] Christelle Hureau,*[,†,‡] and Peter Faller*[,†,‡]

[†]Laboratoire de Chimie de Coordination (LCC), CNRS, 205 route de Narbonne, 31077 Toulouse, France

[‡]LCC, Université de Toulouse, UPS, INPT, 31077 Toulouse, France

[§]Synchrotron SOLEIL, L'Orme des merisiers BP48, Saint-Aubin, F-91192 Gif-Sur-Yvette Cedex, France

Supporting Information

ABSTRACT: Supramolecular assembly of peptides and proteins into amyloid fibrils is of multifold interest, going from materials science to physiopathology. The binding of metal ions to amyloidogenic peptides is associated with several amyloid diseases, and amyloids with incorporated metal ions are of interest in nanotechnology. Understanding the mechanisms of amyloid formation and the role of metal ions can improve strategies toward the prevention of this process and enable potential applications in nanotechnology. Here, studies on Zn^{II} binding to the amyloidogenic peptide Aβ11-28 are reported. Zn^{II} modulates the Aβ11-28 aggregation, in terms of kinetics and fibril structures. Structural studies suggest that Aβ11-28 binds Zn^{II} by amino acid residues Glu11 and His14 and that Zn^{II} is rapidly exchanged between peptides. Structural and aggregation data indicate that Zn^{II} binding induces the formation of the dimeric $Zn^{II}_1(A\beta 11\text{-}28)_2$ species, which is the building block of fibrillar aggregates and explains why Zn^{II} binding accelerates Aβ11-28 aggregation. Moreover, transient Zn^{II} binding, even briefly, was enough to promote fibril formation, but the final structure resembled that of apo-Aβ11-28 amyloids. Also, seeding experiments, i.e., the addition of fibrillar $Zn^{II}_1(A\beta 11\text{-}28)_2$ to the apo-Aβ11-28 peptide, induced aggregation but not propagation of the $Zn^{II}_1(A\beta 11\text{-}28)_2$-type fibrils. This can be explained by the dynamic Zn^{II} binding between soluble and aggregated Aβ11-28. As a consequence, dynamic Zn^{II} binding has a strong impact on the aggregation behavior of the Aβ11-28 peptide and might be a relevant and so far little regarded parameter in other systems of metal ions and amyloidogenic peptides.

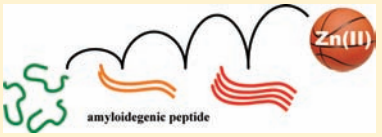

1. INTRODUCTION

The supramolecular assembly of peptides and proteins into amyloid fibrils is intensively studied not only because of their important biological roles in several diseases[1,2] but also because nonpathological roles have been identified.[3] Moreover, amyloids are of interest in nanostructure fabrication and biotechnology.[4,5] Amyloids refer to peptides and proteins that adopt fibrils based on the cross-β structure, in which the peptide backbone is orthogonal to the fibril axis.[4,6,7] They normally form by a two-step process with a slow nucleation phase, followed by a typically fast, autocatalytic surface growth, leading to a sigmoid curve characteristic of amyloid formation, often monitored by thioflavin T (ThT) fluorescence.[8] Binding of metal ions to amyloidogenic peptides is of biological relevance in several cases, including Prion diseases, Alzheimer's disease, Parkinson's disease, amyotrophic lateral scleroses, and type II diabetes, in which specific amyloidogenic peptides or proteins interact with metal ions such as Zn, Cu, Fe, etc.,[9−16] and for which compounds are developed to suppress the effect of the metal ion.[16−21] Also, for biotechnological application or in nanoscience, amyloid fibrils with embedded metal ions are of interest because they can undergo electron-transfer reactions or can serve as catalytic centers.[22−27]

Truncated peptides have been used to model the aggregation of native peptides or to gain general insight into the mechanisms of the aggregating process as well as for nanostructure fabrication.[28] Also, de novo designed peptides were very useful for understanding aggregation and for obtaining nanostructures of the amyloid type.[4,29,30] The interaction of small or truncated amyloidogenic peptides with various metal ions has been studied in the past.[31−37] Recently, we investigated the impacts of stoichiometric Zn^{II} and Cu^{II} binding on three different amyloidogenic model peptides including Aβ11-28 and found metal- and peptide-specific effects related to the coordination chemistry of the metal ions.[38,39] Aβ11-28 is derived from amyloid-β (Aβ) peptide, which plays a central role in Alzheimer's disease. Although Aβ11-28 is missing the N- and C-terminal parts and, hence, is clearly different from Aβ in terms of aggregation and metal binding, it retains two important features for metal-induced amyloid formation. These are the hydrophobic core (amino acid residues spanning from 17 to 21, sequence LVFFA) and the two His residues (His13 and His14) known to anchor the Zn^{II} ion. Thus, this amyloidogenic Aβ11-28 peptide can serve as a model system to gain general insight into metal-induced amyloid formation but does not mimic the special case of native Aβ (although native truncated forms starting from amino acid 11 have been identified in AD[40]).

So far, studies of the effect of metal binding on amyloid formation have focused on the addition of metal ions at the beginning of the aggregation process with the idea that they bind very rapidly[41,42] and stay bound. Only one case is reported

Received: October 17, 2011
Published: December 13, 2011

   dx.doi.org/10.1021/ic202247m | *Inorg. Chem.* 2012, 51, 701−708

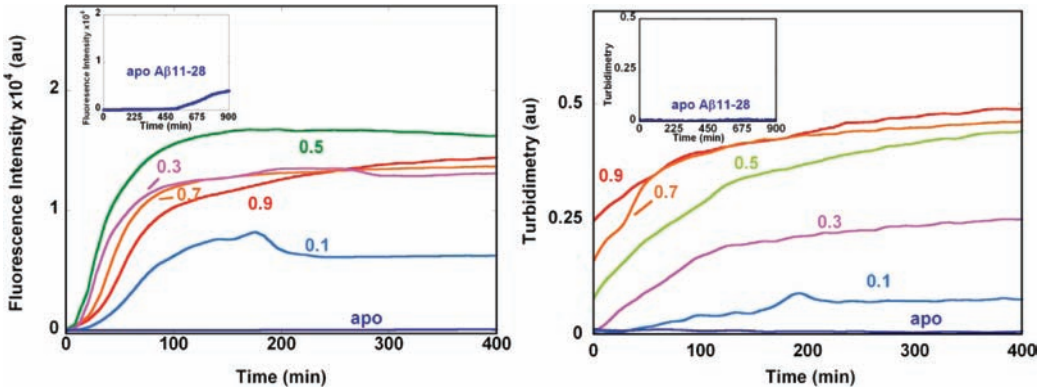

Figure 1. Time-course measurements of ThT fluorescence (left) and turbidity (right) of Aβ11-28 peptide in the presence of Zn^{II}, with Zn^{II} to Aβ11-28 ratios ranging from 0 to 0.9. Conditions: [Aβ11-28] = 300 μM; [Zn^{II}] = 0–270 μM; [HEPES buffer] = 100 mM, pH 7.4; [ThT] = 10 μM. Insets: time-course measurements of ThT fluorescence (left) and turbidity (right) of Aβ11-28 peptide without Zn^{II} (i.e., apo-Aβ11-28) over a longer period.

where transient copper(II) binding to β-2 microglobulin in a 2:1 ratio was sufficient to promote amyloid formation. Copper(II) binding to the natively structured protein β-2 microglobulin induced a conformational change to form an oligomerization-prone structure by exposing a previously buried region. The structural conversion is Cu^{II}-dependent, while the subsequent formation of amyloids is not. The transient copper(II) binding required for conformational change was on the hour time scale.[14,43]

Transient metal ion binding might be of biological relevance because in several biological environments metal-ion concentrations can fluctuate at different time scales; i.e., binding can be dynamic. A well-known example is the Zn^{II} ion in certain glutamatergic neurons, in which Zn^{II} is released in high amounts (up to 300 μM) in the synaptic cleft and taken up in a few seconds.[44,45] Thus, we investigated also dynamical aspects of Zn^{II} binding to the Aβ11-28 model peptide during aggregation, and the results suggest that dynamics can play an important role in the aggregating process and might be of biological relevance.

2. RESULTS

2.1. Aggregation Dependence of the Zn^{II} to Aβ11-28 Ratio. The stoichiometry between metal ions and amyloidogenic peptides can influence the aggregation behavior because of the formation of different types of complexes. Here, the aggregation kinetics were followed by ThT fluorescence and turbidity as a function of the Zn^{II} to Aβ11-28 ratio (Figure 1). ThT is a specific fluorescence dye for amyloid-type aggregates, while turbidity measures all types of aggregates. The Zn^{II} to Aβ11-28 stoichiometry had a pronounced impact on the aggregation behavior, and different changes in the ThT fluorescence and turbidity were observed (Figure 1). The turbidity increased rapidly upon Zn^{II} addition to Aβ11-28. Zn^{II} addition to the buffer only (no peptide) did not show turbidity, hence ruling out that turbidity is due to Zn^{II} precipitation. Increasing the equivalent of Zn^{II} per Aβ11-28 from 0 to 0.9 led to faster kinetics and a higher plateau, a behavior that has often been observed for amyloidogenic peptides (Figure 1, right panel). In contrast, ThT traces did not parallel the one measured by turbidity. The increase in ThT fluorescence was slower and showed the typical sigmoid curve for amyloid-type aggregation due to a nucleation and elongation mechanism.[8] The fastest curve with the most intense plateau was observed for approximately 0.5 equiv of Zn^{II} per Aβ11-28; below and above this stoichiometry, the kinetics and intensity were slower and smaller, respectively (Figure 1, left panel). Turbidity evolved much faster than ThT fluorescence for all Zn^{II} to Aβ11-28 stoichiometries. This indicates that in a first stage ThT-negative amorphous aggregates were formed, which later evolved toward ThT-positive amyloid-like aggregates. During this change, the turbidity intensity stayed more or less constant, suggesting a transformation of the aggregates. This indicates that from 0 to 0.9 equiv of Zn^{II} per Aβ11-28 global aggregation is accelerated and increased, while for fibril formation, 0.5 equiv is the optimum. This can be explained in the most straightforward manner by assuming that a dimeric complex with one Zn^{II} bound to two Aβ11-28 peptides, i.e. $Zn^{II}_1(A\beta 11\text{-}28)_2$, is the building block of the fibrillar-type aggregate. The further addition of Zn^{II} enhanced the formation of aggregates but diminished the fibrillar content, likely by precipitating the $Zn^{II}_1(A\beta 11\text{-}28)_2$ complex via Zn^{II} bridging of two $Zn^{II}_1(A\beta 11\text{-}28)_2$ moieties.

It is important to note that after longer incubation apo-Aβ11-28 aggregated as well (Figure 1, insets) but with different characteristics. Apo-Aβ11-28 reached a plateau of ThT fluorescence approximately 5 times lower than the one observed in the case of $Zn^{II}_{0.5}$-Aβ11-28 and did not show any detectable increase in the turbidity. This strongly indicates that apo-Aβ11-28 forms a different type of amyloid compared to $Zn^{II}_{0.5}$-Aβ11-28. Indeed, transmission electron microscopy (TEM) showed a dense scaffold of fibrillar aggregates for $Zn^{II}_{0.5}$-Aβ11-28, whereas apo-Aβ11-28 formed more isolated fibrillar aggregates (Figure 2).

2.2. Effect of Ethylenediaminetetraacetic Acid (EDTA) on $Zn^{II}_{0.5}$-Aβ11-28. In order to see whether Zn^{II} is involved in the different phases of the aggregation process and if the effect of Zn^{II} binding on Aβ11-28 is reversible, we added the very strong Zn^{II} chelator EDTA (dissociation constant of approximately 10^{-13} M at pH 7.4 compared to approximately 10^{-6} M for Aβ peptide and truncated forms similar to Aβ11-28[46,47]) at different time points. EDTA has been shown to be useful to reverse the effect of Zn^{II} on amyloid formation, like in the case of Aβ1-42, where it abolished completely the inhibitory effect of Zn^{II} on fibril formation.[48] First, as a control, EDTA (5 equiv per Zn^{II} ion) was added just before Zn^{II} and, as expected, the Aβ11-28 aggregation behavior was very similar to that of apo-Aβ11-28, indicating that the Zn^{II}EDTA complex does not interfere with aggregation. Very interestingly, adding EDTA at any time point after the Zn^{II} addition (2 min to 3 h; see Figure S1 in the Supporting Information) did not completely reverse the aggregation profile back to the level of the nonaggregated apo-Aβ11-28 in ThT fluorescence (Figure 3). In other words,

dx.doi.org/10.1021/ic202247m | Inorg. Chem. 2012, 51, 701–708

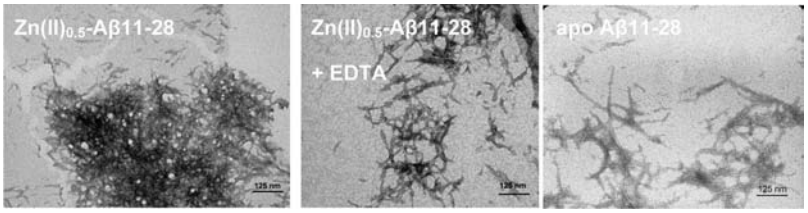

Figure 2. TEM images of $Zn^{II}_{0.5}$-Aβ11-28 (left), $Zn^{II}_{0.5}$-Aβ11-28 + EDTA (middle), and apo-Aβ11-28 (right) after 1 day of incubation. Conditions: [Aβ11-28] = 300 μM; [Zn^{II}] = 0 or 150 μM; [EDTA] = 750 μM; [HEPES buffer] = 100 mM, pH 7.4; [ThT] = 10 μM.

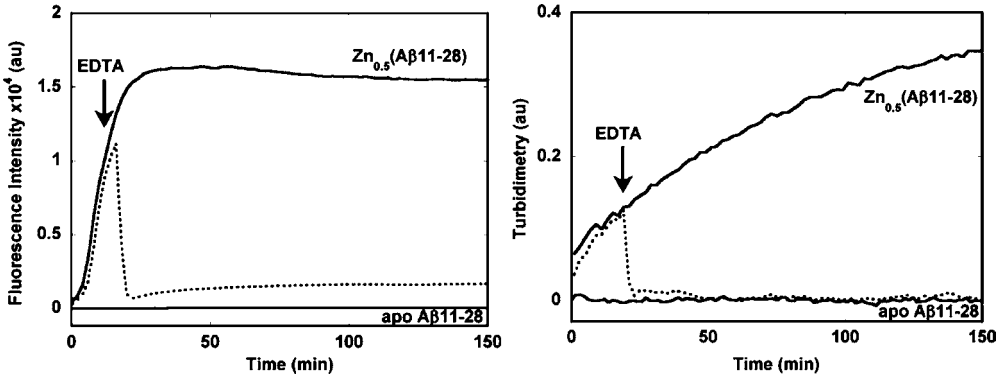

Figure 3. Time course of ThT fluorescence (left) and turbidity (right) of apo-Aβ11-28 and $Zn^{II}_{0.5}$-Aβ11-28 without (solid) and with the addition of EDTA at the time point indicated by the arrow (dashed). Conditions: [Aβ11-28] = 300 μM; [Zn^{II}] = 0 or 150 μM; [EDTA] = 750 μM; [HEPES buffer] = 100 mM, pH 7.4; [ThT] = 10 μM.

the addition of EDTA does not totally reverse the system, and hence even transient Zn^{II} binding is sufficient to induce aggregation. In Figure 3, we are reminded of the fact that apo-Aβ11-28 did not undergo any increase in ThT fluorescence (left panel) or turbidity (right panel) over several hours, while $Zn^{II}_{0.5}$-Aβ11-28 showed the typical sigmoid behavior in ThT fluorescence and a turbidity increase from the beginning. The addition of EDTA to the $Zn^{II}_{0.5}$-Aβ11-28 mixture led to an immediate drop of the turbidity back to the nonaggregated apo-Aβ11-28 level (Figure 3, right). Interestingly, ThT fluorescence did not drop as fast as the turbidity (and sometimes even continued to increase for a while before dropping; data not shown; Figure S1 in the Supporting Information) nor did it drop back to the level of nonaggregated apo-Aβ11-28. At the end, the plateau reached a level similar to that of aggregated apo-Aβ11-28 (compare the left panel in Figure 3 and the inset of the left panel in Figure 1). On the basis of the formation of two types of aggregates, i.e., $Zn^{II}_{0.5}$-Aβ11-28, which exhibits an intense turbidity and high ThT fluorescence, and apo-Aβ11-28, which shows a low ThT fluorescence intensity and no detectible turbidity, the addition of EDTA to $Zn^{II}_{0.5}$-Aβ11-28 resulted in the formation of apo-Aβ11-28-type aggregates, which was much faster compared to that of apo-Aβ11-28 only. This is in line with TEM data (Figure 2), which showed similar types of aggregates for apo-Aβ11-28 and $Zn^{II}_{0.5}$-Aβ11-28 plus EDTA (more isolated fibrillar-type structures), but different from Zn^{II}-Aβ11-28 (more dense).

The addition of EDTA to $Zn^{II}_{0.5}$-Aβ11-28 at different time points did not change the overall feature; i.e., shorter or longer transient Zn^{II} binding modulated the aggregation behavior compared to apo-Aβ11-28 in any case (see Figure S1 in the Supporting Information). There were variations in the kinetics and intensity of the drop of ThT fluorescence, but in all experiments, the decrease of ThT fluorescence was slower than that of turbidity. Moreover, at the end, the fluorescence intensity was similar to that of the aggregated apo-Aβ11-28 peptide (Figure 1, left inset) but was reached much faster (Figure S1 in the Supporting Information). This indicates that Zn^{II} is able to nucleate the amyloid formation of apo-Aβ11-28, even when it binds only transiently.

Aβ11-28, after Zn^{II} and EDTA treatments, aggregates faster than without such treatments. Thus EDTA does not reverse $Zn^{II}_{0.5}$-Aβ11-28 back to nonaggregated apo-Aβ11-28 (Figure 3). This indicates that, after Zn^{II} removal by EDTA, apo-Aβ11-28 is in a different state (likely an oligomeric form) and is more prone to aggregation than monomeric apo-Aβ11-28 (Scheme 1).

To see the effect of Zn^{II} addition to aggregated apo-Aβ11-28 (formed via EDTA-treated $Zn^{II}_{0.5}$-Aβ11-28), Zn^{II} was added again at a concentration equal to that of EDTA, leading to Zn^{II}EDTA and $Zn^{II}_{0.5}$-Aβ11-28 species. ThT fluorescence increased again with a sigmoidal curve similar to that observed in the case of Zn^{II} addition to monomeric apo-Aβ11-28 (Figure 4). This can be most straightforwardly explained assuming that Zn^{II} induces aggregation of a portion of the soluble apo-Aβ11-28 peptide. Because of equilibrium between the aggregated and soluble states in amyloids, aggregated apo-Aβ11-28 is solubilized into monomeric Aβ11-28, leading to further Zn^{II}-induced aggregation. Thus, the aggregated apo-Aβ11-28 is transformed into aggregated $Zn^{II}_{0.5}$-Aβ11-28 (Scheme 1).

2.3. Seeding Experiment and Labile Zn^{II} Binding. Because the previous experiments indicated that two structural different aggregates are formed for apo- and $Zn^{II}_{0.5}$-Aβ11-28, we tested if aggregated $Zn^{II}_{0.5}$-Aβ11-28 can seed apo-Aβ11-28. Indeed, after seeding of soluble apo-Aβ11-28 with 7.5% preaggregated $Zn^{II}_{0.5}$-Aβ11-28, ThT fluorescence immediately started to increase and reached a plateau of intensity similar to that of apo-Aβ11-28 (Figure 5, left). No increase in the turbidity was detected (Figure 5, right). This indicates that indeed $Zn^{II}_{0.5}$-Aβ11-28 can nucleate aggregation of apo-Aβ11-28, but the aggregates formed are of the apo-type, so it is a triggering rather

dx.doi.org/10.1021/ic202247m | Inorg. Chem. 2012, 51, 701−708

Scheme 1. Monomeric Aβ11-28 Peptide (Triangles) Binding Zn^{II} (Red Circles) and Forming $Zn^{II}_1(Aβ11\text{-}28)_2$[a]

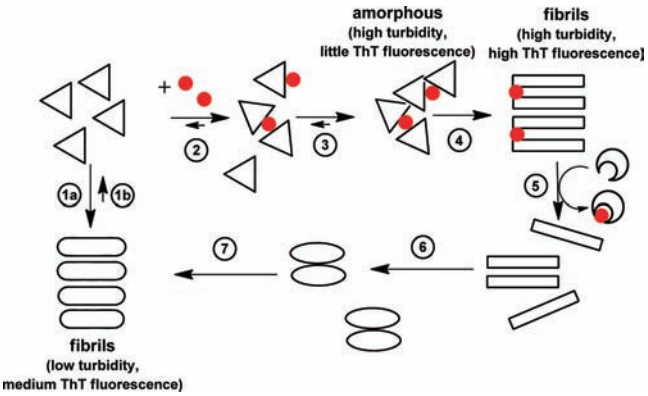

[a] $Zn^{II}_1(Aβ11\text{-}28)_2$ rapidly form amorphous-type aggregates (triangles) with high turbidity and very little ThT fluorescence, which then evolve into amyloid-type aggregates (rectangular sticks). The addition of EDTA (open rings) does not reverse the system to monomeric Aβ11-28 (triangles) but induces a form with a different conformation (ellipses) more prone to aggregate into apo-Aβ11-28 amyloid-type fibrils (round sticks).

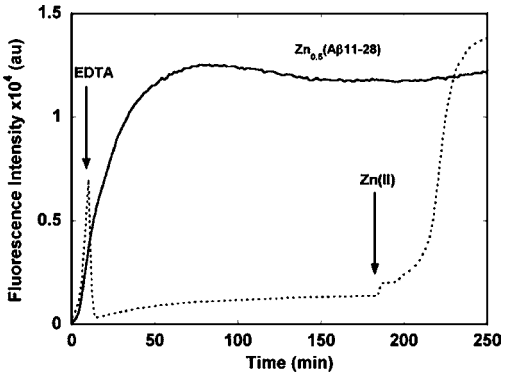

Figure 4. Time course of ThT fluorescence of $Zn^{II}_{0.5}$-Aβ11-28 (solid) and of $Zn^{II}_{0.5}$-Aβ11-28 with the addition of EDTA after ~10 min and of Zn^{II} after ~190 min (dashed). Conditions: [Aβ11-28] = 300 μM; [Zn^{II}] = 150 and 900 μM (after 190 min); [EDTA] = 750 μM; [HEPES buffer] = 100 mM, pH 7.4; [ThT] = 10 μM.

than a seeding effect because the structure of the seed is not propagated (Scheme 2).

Scheme 2. Model for the Triggering of apo-Aβ11-28 (Triangles) with Amyloid-Type Aggregates of $Zn^{II}_{0.5}$-Aβ11-28 (Zn^{II}, Red Circles; Peptides, Rectangular Sticks; See Also Scheme 1)[a]

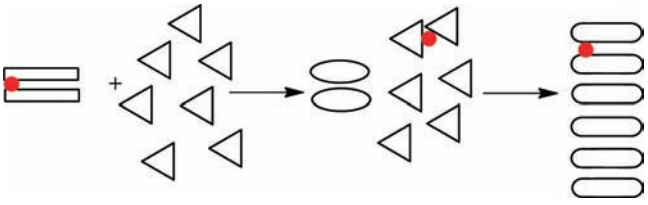

[a] The structure of $Zn^{II}_{0.5}$-Aβ11-28 is not propagated like in a "seeding" process, but Zn^{II} triggers aggregation of monomeric apo-Aβ11-28 to amyloid-type apo-Aβ11-28 (round sticks) because of its fast exchange between the different forms of Aβ11-28 (see also Scheme 1).

The model shown in Scheme 2 is based on a fast exchange of Zn^{II} between peptides. NMR experiments with several amyloid-type peptides indicated that exchange of Zn^{II} between the peptides is faster than that on the NMR time scale (approximately milliseconds).[49−51] This is also the case for the Aβ11-28 peptide because the substoichiometric addition of Zn^{II} affects the resonances of the entire sample (see below and Figure S2 in the Supporting Information). To see if the predicted fast exchange is also possible for the aggregated $Zn^{II}_{0.5}$-Aβ11-28, the Zn^{II}-sensitive chelator 4-(2-pyridylazo)resorcinol (PAR) was used (Figure 6). PAR forms the Zn^{II} complex $[Zn^{II}(PAR)_2]$, which absorbs at λ = 490 nm with $\varepsilon = 73 \times 10^3\ M^{-1}\ cm^{-1}$, while PAR alone absorbs at λ = 413 nm ($\varepsilon = 33 \times 10^3\ M^{-1}\ cm^{-1}$).[52] PAR was able to retrieve Zn^{II} very rapidly and quantitatively (half-time faster than 1 min), indicating indeed that Zn^{II} in aggregated $Zn^{II}_{0.5}$-Aβ11-28 is very labile and suggesting that Zn^{II} exchange between aggregated and soluble Aβ11-28 is also quite rapid. Hence, Zn^{II} in aggregates could have an impact on the aggregation of soluble apo-Aβ11-28 via fast Zn^{II} exchange reactions.

2.4. X-ray Absorption Spectroscopy (XAS). In order to obtain structural information about Zn^{II} binding to Aβ11-28, X-ray absorption near-edge structure (XANES) was used. XANES experiments with 0.5 and 1.0 equiv of Zn^{II} per Aβ11-28 peptide were performed at the beginning and at the end of the aggregation process (Figure 7). All of the spectra are in line with a mononuclear Zn^{II} site and resemble most proteins with tetracoordinated Zn^{II} including two His residues.[53,54]

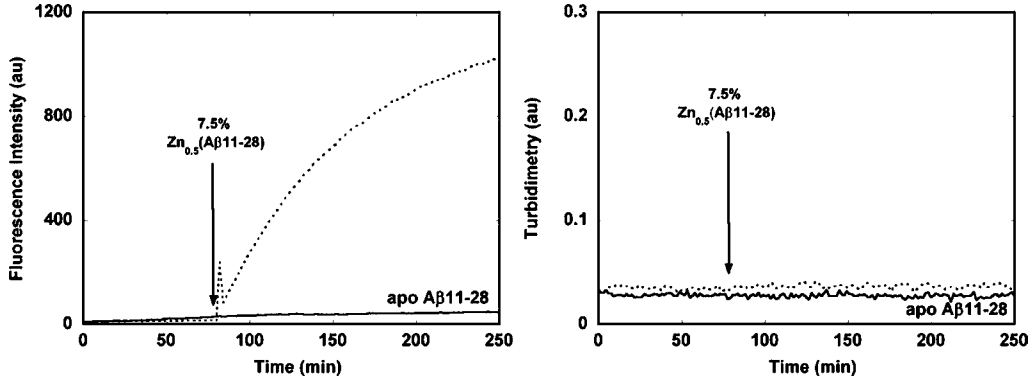

Figure 5. Time course of ThT fluorescence (left) and turbidity (right) of apo-Aβ11-28 without (solid) and with the addition of 7.5% preaggregated $Zn^{II}_{0.5}$-Aβ11-28 (dashed). Conditions: [Aβ11-28] = 300 μM; [$Zn^{II}_{0.5}$-Aβ11-28] = 22.5 μM added after 90 min (indicated by an arrow); [HEPES buffer] = 100 mM, pH 7.4; [ThT] = 10 μM. The addition of preaggregated $Zn^{II}_{0.5}$-Aβ11-28 is indicated by an arrow.

dx.doi.org/10.1021/ic202247m | Inorg. Chem. 2012, 51, 701−708

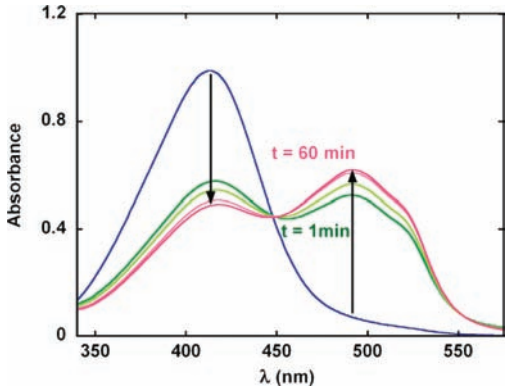

Figure 6. UV−vis monitoring of the addition of preaggregated $Zn^{II}_{0.5}$-Aβ11-28 to PAR. [PAR] = 300 μM; preaggregated [$Zn^{II}_{0.5}$-Aβ11-28] = 160 μM; [Zn^{II}] = 80 μM; [HEPES] = 100 mM, pH 7.4.

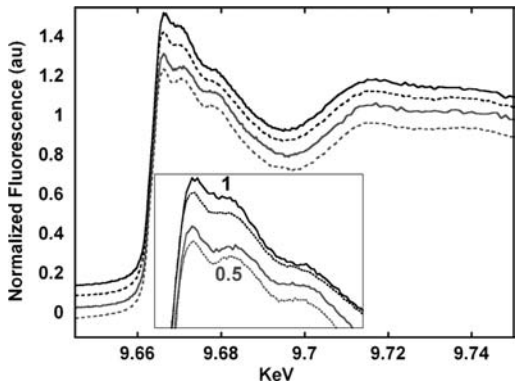

Figure 7. XANES spectra of $Zn^{II}_{0.5}$-Aβ11-28 (gray, **0.5**) and Zn^{II}_{1}-Aβ11-28 (black, **1**) before (dashed) and after (solid) aggregation at pH 7. Inset: magnification of the zone around 9.67 keV. [Aβ11-28] = 2.4 mM; [Zn^{II}] = 1.2 or 2.2 mM; [HEPES] = 50 mM, pH 7.0.

No difference between the beginning and end of the aggregation was observed, indicating that the coordination sphere does not change much during aggregation. The spectra were slightly different compared to previous measurements of Zn^{II}_{1}-Aβ11-28 at pH 8.6, indicating a pH-dependent Zn^{II} coordination.[38]

The measurements at different stoichiometries, i.e., $Zn^{II}_{0.25}$-Aβ11-28, $Zn^{II}_{0.5}$-Aβ11-28, and Zn^{II}_{1}-Aβ11-28, supported the formation of the dimeric Zn^{II}_{1}(Aβ11-28)$_2$ species because Aβ11-28 species with 0.25 and 0.5 equiv of Zn^{II} were identical, but with 1 equiv, features were dampened. This points to a more homogeneous coordination site of the first 0.5 equiv of Zn^{II}, in contrast to a more heterogeneous binding of the second 0.5 equiv of Zn^{II}. This is in line with formation of the dimeric Zn^{II}_{1}(Aβ11-28)$_2$ complex as a building block.

2.5. NMR. As shown by XANES, Zn^{II} coordination does not change significantly during aggregation, suggesting that Zn^{II} binding in the soluble state, as can be probed by NMR, is also relevant for the aggregated state. Hence, the effect of the Zn^{II} addition of the Aβ11-28 peptide was monitored by NMR (Figures 8 and S2−S4 in the Supporting Information). Zn^{II} induced line broadening and chemical shifts of some specific resonances. Figure 8 shows the aromatic region of the ^{1}H NMR spectra of the Aβ11-28 peptide in the absence and presence of 1 equiv of Zn^{II}, including the two His and two Phe residues. Zn^{II} addition leads to line broadening and a shift of only one of the two H_δ and only one of the two H_ε of His13 or His14. The other H_δ and H_ε resonances are only weakly affected, likely

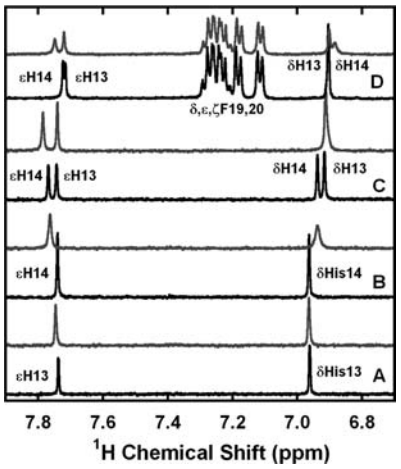

Figure 8. ^{1}H NMR of apo- (lower black trace) and Zn^{II} peptides (upper gray trace) of EVHG (A), EVRH (B), EVHH (C), and Aβ11-28 (D). Conditions: [peptide] = 300 μM; [Zn^{II}] = 270 μM; [Tris-d^{11}] = 100 mM, pH 7.5.

because of perturbation by Zn^{II} binding to the neighboring His. The resonances of the two Phe residues are not affected at all, indicating no binding to or near the Phe residues. The other affected residues were Glu11 and Val12 (see Figures S3 and S4 in the Supporting Information). This is attributed to the involvement of Glu11 in Zn^{II} binding, with Val12 being affected because of its vicinity to Glu11.

Because Aβ11-28 aggregation precluded the attribution of the resonances by longer NMR measurements (2D and ^{13}C experiments), we used model peptides corresponding to the Zn^{II}-binding region Glu-Val-His-His (EVHH-NH_2). Upon Zn^{II} addition to the EVHH peptide, although with slight differences, the Zn^{II} effect observed on the Aβ11-28 spectrum was reproduced, i.e., one of the His is much more affected than the other one (Figure 8C,D). The addition of Zn^{II} to the EVHG peptide lacking the His14 residue did not perturb significantly the NMR spectrum, with the remaining His13 being only weakly affected (Figure 8A). This indicates that the Zn^{II} binding His is His14. This was confirmed by the study of the EVRH peptide lacking His13, in which His14 is affected similarly to the His14 from Aβ11-28 (Figure 8B,D). This allowed assignment of the highly affected His of Aβ11-28 to His14. Moreover, a comparison between the EVHH and Aβ11-28 spectra in the Glu11 H_β and H_γ regions with and without Zn^{II} established the implication of Glu11 in Zn^{II} binding (Figure S4 in the Supporting Information). This agrees with the recent work of Kozin and collaborators, who proposed binding of Zn^{II} to COO^- of Glu11 and to His14 in the peptide Ac-Glu-Val-His-His-NH_2 with an apparent K_d in the lower micromolar range.[47,55] In conclusion, Zn^{II} binds preferentially to Glu11 (COO^-) and His14 in Aβ11-28 (Scheme 3). These structural features are fully in line with the possible formation of a dimeric Zn^{II}_{1}(Aβ11-28)$_2$ species, as indicated by the aggregation experiments (see above).

3. DISCUSSION

The structural studies described above suggest that Zn^{II} binds to Glu11 (COO^-) and His14 and that a dimeric Zn^{II}_{1}(Aβ11-28)$_2$ can be formed in line with recent studies on Ac-EVHH-NH_2.[47,55] These dimers are likely to be formed transiently and dynamically and aggregated further to larger aggregates.

dx.doi.org/10.1021/ic202247m | Inorg. Chem. 2012, 51, 701−708

Scheme 3. Model of the $Zn^{II}_1(A\beta 11\text{-}28)_2$ Complex[a]

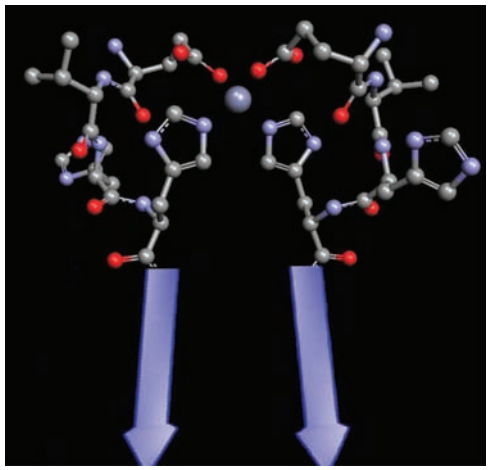

[a]Shown are Glu11, Val12, His13, and His14. Gln15 to Lys28 are represented as arrows. Zn^{II} is bound by Glu11 (COO^-) and His14 of Aβ11-28. Other ligands are possible (e.g., H_2O).

Amyloid-type fibrils are most rapidly and most intensively formed at 0.5 Zn^{II} per Aβ11-28 ratio, suggesting that the dimer $Zn^{II}_1(A\beta 11\text{-}28)_2$ is the building block of fibrils. This is supported by considering the overall charge. Classically, proteins precipitate and often aggregate into amyloids better when the net charge is smaller. At pH 7.4, apo-Aβ11-28 has a charge of 1−. The $Zn^{II}(A\beta 11\text{-}28)$ complex is thus expected to have 1+ charge, while $Zn^{II}_1(A\beta 11\text{-}28)_2$ has an expected charge of 0 and thus fits better with the faster aggregation. Further Zn^{II} addition decreased fibril formation but increased the turbidity, likely because of binding of Zn^{II} between the $Zn^{II}_1(A\beta 11\text{-}28)_2$ units and subsequent distortion of the amyloid-like aggregation of the $Zn^{II}_1(A\beta 11\text{-}28)_2$ units with the formation of more amorphous-like aggregates.

A very important finding is that Zn^{II} binding is very dynamic and Zn^{II} exchange between soluble and aggregated Aβ11-28 is rapid, which has a crucial impact on the aggregation behavior (Schemes 1 and 2). Apo-Aβ11-28 aggregates into amyloid-type fibrils with moderate ThT fluorescence and very little turbidity because the fibrils are not clumped together (Scheme 1, process 1a). Zn^{II} binding to apo-Aβ11-28 is rapid (Scheme 1, process 2) and forms at least transiently a dimeric $Zn^{II}_1(A\beta 11\text{-}28)_2$ complex, which forms amorphous-type aggregates (Scheme 1, process 3) with intense turbidity but no ThT fluorescence. These aggregates evolve toward amyloid-type fibrils (high ThT fluorescence), forming dense meshes (therefore, high turbidity). If Zn^{II} is added to preaggregated apo-Aβ11-28, the same process likely occurs (Scheme 1, processes 2−4) and soluble apo-Aβ11-28 is repopulated by the dissolution of aggregated apo-Aβ11-28 (process 1b). In contrast, when EDTA is added to Zn^{II}-Aβ11-28 aggregates (process 5), apo-Aβ11-28 aggregates are formed but not via the reversed pathway (processes 4 to 2). Instead another pathway is taken (Scheme 1, processes 5−7). This is supported by the findings that the turbidity is dropping faster than ThT fluorescence, indicating an intermediate state and that formation of apo-Aβ11-28 is much faster than expected from a reversible pathway.

As a consequence, transiently adding Zn^{II} to apo-Aβ11-28 results in fibrils like the ones formed by apo-Aβ11-28 only but dramatically accelerates formation. Transient Zn^{II} binding over different time periods shows the effect, but a period of transient Zn^{II} binding of less than 1 min is sufficient to accelerate the formation of apo-Aβ11-28 aggregates. This clearly shows that transient Zn^{II} binding in the second time scale can have a nucleation effect on the aggregation of apo-Aβ11-28. Moreover, transient Zn^{II} binding accelerates the formation of apo-Aβ11-28 at substoichiometric amounts (Figure 1), showing that relatively low concentrations of Zn^{II} can have an important effect on aggregation. The dynamic exchange of Zn^{II} binding to Aβ11-28 did not only involve soluble Aβ11-28 because aggregated Zn^{II}-Aβ11-28 was also able to take part in the exchange. The observation that the addition of a small fraction of preaggregated $Zn^{II}_{0.5}$-Aβ11-28 to soluble apo-Aβ11-28 ("seeding experiment") forms apo-type aggregates and not Zn^{II}-type aggregates is in line with nucleation due to Zn^{II} exchange (see above).

These new findings about the very dynamic Zn^{II} exchange between different forms of Aβ11-28 might also apply to other systems with metal ion and amyloidogenic peptide interactions and have the following important impacts:

i. Transient Labile Metal Pools. Fast transient Zn^{II} binding might be very relevant for certain biological systems, in particular for the Aβ peptide and Zn^{II} in Alzheimer's disease. In certain synapses, Zn^{II} is ejected in the synaptic cleft and taken up on the second time scale[44,45] and plays the role of a neuromodulator. This Zn^{II} has been shown to be involved in the formation of Aβ deposits, and the distribution of histological stainable Zn^{II} resembles the area most prone to amyloid deposit in Alzheimer's disease.[56] Moreover, in vitro Zn^{II} is able to induce Aβ aggregation in milliseconds.[41] A similar transient increase of the metal-ion concentration in certain synaptic clefts has been proposed for copper.[57−59] Another example is the release of Zn^{II} from pancreatic islet β cells into the blood, which includes locally high Zn^{II} concentrations next to the release before dilution out in the blood.[15,16]

ii. Trace Metal Ions. It has been observed, for different metal−amyloidogenic interactions, that trace amounts (large substoichiometric) of metal ions can have a strong impact on aggregation.[60−63] This has classically been assigned to the induction of a stable metal−peptide nucleus with a further elongation phase consisting of apo-peptide addition to the nucleus. The dynamic exchange found here sheds more light on the mechanism: substoichimetric amounts of metal ions will not be bound to a portion of the peptide in a stable 1:1 complex but can be exchanged and thus bound transiently to the entire pool of peptides. Hence, metal ions induce nucleation of a much higher peptide concentration compared to its concentration,and this in a relatively short time.

iii. Binding Constant. For several biological relevant systems of metal−peptide interactions (Aβ, prion, α-synuclein, amylin, etc.), the binding affinity for metal ions is much weaker than that for classical metalloproteins (see, e.g., refs 12, 23, and 64−67), and hence sometimes the biological relevance of metal binding to these peptides has been questioned. However, in light of the present findings, a strong affinity is not required because a substoichiometric amount of transiently bound metal ions is sufficient for having a high impact on the aggregation behavior.

iv. Metal-Ion Source. The dynamic exchange of Zn^{II} binding to Aβ11-28 did not only involve the soluble Aβ11-28 because aggregated Zn^{II}-Aβ11-28 was also able to take part in the exchange. This means that metal−peptide aggregates can provide metal ions for transient binding to soluble apo peptide. This might be particularly relevant for Aβ, where amyloid

dx.doi.org/10.1021/ic202247m | Inorg. Chem. 2012, 51, 701−708

plaques contain a high amount of metal ions available for metal binding by external chelators.[46,68] Moreover, metal ions could also originate from other biomolecules containing labile-bound metal ions, like metallothioneins.[69]

In conclusion, modulators of amyloid formation can interact differently, i.e., covalently, by coordination, or by weak interactions. For the latter two, transient binding is possible. Binding of metal ions has been reported for quite a lot of amyloidogenic proteins/peptides, and in several cases, they seem to be biologically relevant. So far, not that much attention has been paid to dynamic exchange reactions, in particular related to aggregation species. The studies of our model system revealed that dynamic metal exchange reactions between soluble and aggregated peptides are an important mechanism that can strongly impact the aggregation behavior.

4. MATERIALS AND METHODS

Aβ11-28 Sample Preparation. The peptide Aβ11-28 (sequence Glu-Val-His-His-Gln-Lys-Leu-Val-Phe-Phe-Ala-Glu-Asp-Val-Gly-Ser-Asn-Lys) was purchased from GenScript Corp. (Piscataway, NJ). The stock solutions of Aβ11-28 (~1.2 mM) have been prepared by dissolving the peptide in Milli-Q water (resistivity = 18 MΩ cm^{-1}) or in D_2O for an NMR stock solution, which resulted in a final pH of 2. The pH of the solution was then adjusted to pH 12 by adding NaOH (or NaOD for NMR) stock solutions, in order to monomerize the peptides. These stock solutions were stored at 253 K. The peptide concentrations were determined by using the molar extinction coefficient ε = 390 M^{-1} cm^{-1} of the two phenylalanines at 258 nm.[30] Because phenylalanine does not absorb at 275 nm, absorption at that wavelength was subtracted in order to remove contributions from the buffer or baseline drifts. A Zn^{II} stock solution was prepared with $Zn^{II}SO_4$ monohydrate (Strem Chemicals) in water or in D_2O for NMR experiment. Aggregation of peptides in the presence of Zn^{II} has been performed by dissolving peptides from a stock solution in a 100 mM 4-(2-hydroxyethyl)-1-piperazylethanesulfonic acid (HEPES) buffer at pH 7.4 and was controlled at the end of the experiment.

All of the experiments measuring either turbidimetry or fluorescence intensity have been realized at 298 K. The experiments were repeated at least five times in different preparations. There were variations in the kinetics, but the trends shown were always the same. Data shown are representative measurements.

In the XANES measurements, the first sample (t = 0 h) was withdrawn immediately after mixing, transferred to the sample holder, and frozen in liquid nitrogen. The second sample was incubated for 15 h at room temperature before transferring to and freezing in the sample holder.

EDTA. An EDTA solution at 100 mM is prepared from ethylenediaminetetraacetic acid disodium salt (Sigma-Aldrich).

Tetrapeptides. EVHH-NH_2, EVHG-NH_2, and EVRH-NH_2 peptides (N-terminal amine; C-terminal amide) were purchased from GenScript Corp. (Piscataway, NJ). The stock solutions were prepared by dissolving the peptides in D_2O. The peptide concentrations were determined by Cu^{II} titration (see ref 32).

4-(2-Pyridylazo)resorcinol (PAR) Measurement. PAR was purchased from Sigma-Aldrich. UV−vis measurements were done in a 1 mm quartz cuvette in the presence of a HEPES buffer at pH 7.4 (100 mM).[70]

UV−Vis Spectroscopy. UV−vis spectra were recorded on an Agilent 8453 UV−vis spectrometer. Measurements were performed at room temperature.

Turbidimetry. Turbidity measurements were done by measuring the absorbance at 350 nm with a FLUOstar Optima (BMG Labtech) in a quartz microplate (96-well, Hellma).

Fluorescence Spectroscopy. Fluorescence spectra were measured by using a FLUOstar Optima (BMG Labtech). ThT (Acros), Aβ11-28, and Zn^{II} were mixed in a 100 mM HEPES buffer at pH 7.4 and placed in 96-well microplate. The time course of ThT fluorescence was then measured (excitation, 440 nm; emission, 490 nm; bandwidth for emission and excitation, 10 nm). The final concentrations of Aβ11-28 and ThT were 300 and 10 μM, respectively.

TEM. Peptide samples (15 μL) incubated for 17 h were applied on EM grids, washed with 15 μL of Milli-Q water, and negatively stained with an aqueous solution (15 μL) of uranyl acetate (1% w/w). Samples were air-dried and examined with a JEOL 1011 transmission electron microscope operating at an accelerating voltage of 100 kV or on a HU12A transmission electron microscope (75 kV). Conditions: [Aβ11-28] = 300 μM; [Zn^{II2+}] = 0 or 150 μM; [EDTA] = 750 μM; [HEPES buffer] = 100 mM, pH 7.4; [ThT] = 10 μM. EDTA was added after 1 day of incubation and 10 min before grid deposition.

XAS. XANES measurements were carried out at the SOLEIL Synchrotron Facility (St. Aubin, France), which was operating with a ring current of 400 mA. Zn^{II} K-edge XAS spectra were collected on the MARS beamline.[71] The measurements were performed using a Si(220) water-cooled double-crystal monochromator and two large silicon mirrors for high-energy harmonics rejection. Energy calibration was achieved by measuring a copper foil and assigning the first inflection point of the absorption spectrum to 8979 eV. The spectra were measured in fluorescence mode by measuring the Zn^{II} K_α fluorescence with a silicon drift detector (SII Nanotechnology). The liquid samples were injected into special sample holders and cooled to 20−30 K using a helium-flow cryostat. XANES spectra were background-corrected by a linear regression through the preedge region and a polynomial through the postedge region and normalized to the edge jump.

NMR. NMR experiments were realized on a Avance 500 Bruker NMR spectrometer. Aβ11-28 samples were freshly prepared from a D_2O stock solution (see the Aβ11-28 Sample Preparation section). The pH value of Aβ11-28 (300 μM) and a deuterated tris(hydroxymethyl)-aminomethane (Tris) buffer (100 mM) was adjusted to 7.5. The residual water signal was suppressed by a presaturation procedure. Zn^{II} was directly added to the NMR tube, and measurement was performed as quickly as possible (less than 1 min 30 s) in order to minimize the aggregation process during spectrum acquisition. EVHH-NH_2, EVHG-NH_2, and EVRH-NH_2 samples were prepared by diluting stock solutions (see the Tetrapeptide section) to 300 μM in a deuterated Tris buffer (100 mM); the pH value was adjusted to 7.4.

■ ASSOCIATED CONTENT

Ⓢ Supporting Information

Time course of ThT fluorescence and ^1H NMR spectra. This material is available free of charge via the Internet at http://pubs.acs.org.

■ AUTHOR INFORMATION

Corresponding Author

*E-mail: peter.faller@lcc-toulouse.fr (P.F.), christelle.hureau@lcc-toulouse.fr (C.H.). Phone: (+33) 5 61 33 31 62 (P.F.), (+33) 5 61 33 31 62 (C.H.). Fax: (+33) 5 61 55 30 03 (P.F.), (+33) 5 61 55 30 03 (C.H.).

■ ACKNOWLEDGMENTS

Financial support from ANR Neurometals (Agence Nationale de la Recherche Neurometals; Grant NT09-488591) and from "Region Midi-Pyrénées" (Research Grant APRTCN09004783) is acknowledged. We acknowledge SOLEIL for a provision of synchrotron radiation on the MARS beamline (Proposal 20090686).

■ REFERENCES

(1) Haass, C.; Selkoe, D. J. *Nat. Rev. Mol. Cell Biol.* **2007**, *8*, 101−112.
(2) Chiti, F.; Dobson, C. M. *Annu. Rev. Biochem.* **2006**, *75*, 333−366.
(3) Fowler, D. M.; Koulov, A. V.; Balch, W. E.; Kelly, J. W. *Trends Biochem. Sci.* **2007**, *32* (5), 217−224.
(4) Hamley, I. W. *Angew. Chem., Int. Ed.* **2007**, *46* (43), 8128−8147.
(5) Gazit, E. *Chem. Soc. Rev.* **2007**, *36* (8), 1263−1269.

(6) Cherny, I.; Gazit, E. *Angew. Chem., Int. Ed.* **2008**, *47* (22), 4062–4069.
(7) Morris, K.; Serpell, L. *Chem. Soc. Rev.* **2010**, *39* (9), 3445–3453.
(8) Morris, A. M.; Watzky, M. A.; Agar, J. N.; Finke, R. G. *Biochemistry* **2008**, *47* (8), 2413–2427.
(9) Exley, C. *J. Alzheimer's Dis.* **2006**, *10* (2–3), 173–177.
(10) Barnham, K. J.; Cappai, R.; Beyreuther, K.; Masters, C. L.; Hill, A. F. *Trends Biochem. Sci.* **2006**, *31* (8), 465–472.
(11) Tougu, V.; Tiiman, A.; Palumaa, P. *Metallomics* **2011**, *3* (3), 250–261.
(12) Hong, L.; Simon, J. D. *Metallomics* **2011**, *3* (3), 262–266.
(13) Perez, L. R.; Franz, K. J. *Dalton Trans. 39* (9), 2177–2187.
(14) Calabrese, M. F.; Miranker, A. D. *Prion* **2009**, *3* (1), 1–4.
(15) Brender, J. R.; Salamekh, S.; Ramamoorthy, A. *Acc. Chem. Res.* **2011**.
(16) Detoma, A. S.; Salamekh, S.; Ramamoorthy, A.; Lim, M. H. *Chem. Soc. Rev.* **2011**.
(17) Hindo, S. S.; Mancino, A. M.; Braymer, J. J.; Liu, Y.; Vivekanandan, S.; Ramamoorthy, A.; Lim, M. H. *J. Am. Chem. Soc.* **2009**, *131* (46), 16663–16665.
(18) Hureau, C.; Sasaki, I.; Gras, E.; Faller, P. *ChemBioChem* **2010**, *11* (7), 950–953.
(19) Crouch, P. J.; Hung, L. W.; Adlard, P. A.; Cortes, M.; Lal, V.; Filiz, G.; Perez, K. A.; Nurjono, M.; Caragounis, A.; Du, T.; Laughton, K.; Volitakis, I.; Bush, A. I.; Li, Q. X.; Masters, C. L.; Cappai, R.; Cherny, R. A.; Donnelly, P. S.; White, A. R.; Barnham, K. J. *Proc. Natl. Acad. Sci. U.S.A.* **2009**, *106* (2), 381–386.
(20) Bush, A. I.; Tanzi, R. E. *Neurotherapeutics* **2008**, *5* (3), 421–432.
(21) Scott, L. E.; Orvig, C. *Chem. Rev.* **2009**, *109* (10), 4885–4910.
(22) Brown, D. R. *Dalton Trans.* **2009**, *21*, 4069–4076.
(23) Faller, P.; Hureau, C. *Dalton Trans.* **2009**, 1080–1094.
(24) Drago, D.; Bolognin, S.; Zatta, P. *Curr. Alzheimer Res.* **2008**, *5* (6), 500–507.
(25) Fritz, G.; Botelho, H. M.; Morozova-Roche, L. A.; Gomes, C. M. *FEBS J.* **2010**, *277* (22), 4578–4590.
(26) Duce, J. A.; Bush, A. I. *Prog. Neurobiol. 92* (1), 1–18.
(27) Gaggelli, E.; Kozlowski, H.; Valensin, D.; Valensin, G. *Chem. Rev.* **2006**, *106* (6), 1995–2044.
(28) Gazit, E. *Prion* **2007**, *1* (1), 32–35.
(29) Lynn, D. G.; Meredith, S. C. *J. Struct. Biol.* **2000**, *130* (2–3), 153–173.
(30) Eisenberg, D.; Nelson, R.; Sawaya, M. R.; Balbirnie, M.; Sambashivan, S.; Ivanova, M. I.; Madsen, A. O.; Riekel, C. *Acc. Chem. Res.* **2006**, *39* (9), 568–575.
(31) Yang, H.; Pritzker, M.; Fung, S. Y.; Sheng, Y.; Wang, W.; Chen, P. *Langmuir* **2006**, *22* (20), 8553–8562.
(32) Pagel, K.; Seri, T.; von Berlepsch, H.; Griebel, J.; Kirmse, R.; Bottcher, C.; Koksch, B. *ChemBioChem* **2008**, *9* (4), 531–536.
(33) Hoernke, M.; Koksch, B.; Brezesinski, G. *Biophys. Chem.* **2010**, *150* (1–3), 64–72.
(34) Schlosser, G.; Stefanescu, R.; Przybylski, M.; Murariu, M.; Hudecz, F.; Drochioiu, G. *Eur. J. Mass Spectrom. (Chichester, England)* **2007**, *13* (5), 331–337.
(35) Dong, J.; Canfield, J. M.; Mehta, A. K.; Shokes, J. E.; Tian, B.; Childers, W. S.; Simmons, J. A.; Mao, Z.; Scott, R. A.; Warncke, K.; Lynn, D. G. *Proc. Natl. Acad. Sci. U.S.A.* **2007**, *104* (33), 13313–13318.
(36) Dong, J.; Shokes, J. E.; Scott, R. A.; Lynn, D. G. *J. Am. Chem. Soc.* **2006**, *128* (11), 3540–3542.
(37) Scotter, A. J.; Guo, M.; Tomczak, M. M.; Daley, M. E.; Campbell, R. L.; Oko, R. J.; Bateman, D. A.; Chakrabartty, A.; Sykes, B. D.; Davies, P. L. *BMC Struct. Biol.* **2007**, *7*, 63.
(38) Alies, B.; Pradines, V.; Llorens-Alliot, I.; Sayen, S.; Guillon, E.; Hureau, C.; Faller, P. *J. Biol. Inorg. Chem.* **2011**, *16* (2), 333–340.
(39) Pradines, V.; Jurca Stoia, A.; Faller, P. *New J. Chem.* **2009**, *32*, 1189–1194.
(40) Naslund, J.; Schierhorn, A.; Hellman, U.; Lannfelt, L.; Roses, A. D.; Tjernberg, L. O.; Silberring, J.; Gandy, S. E.; Winblad, B.; Greengard, P.; et al. *Proc. Natl. Acad. Sci. U.S.A.* **1994**, *91* (18), 8378–8382.
(41) Noy, D.; Solomonov, I.; Sinkevich, O.; Arad, T.; Kjaer, K.; Sagi, I. *J. Am. Chem. Soc.* **2008**, *130* (4), 1376–1383.
(42) Pedersen, J. T.; Teilum, K.; Heegaard, N. H.; Ostergaard, J.; Adolph, H. W.; Hemmingsen, L. *Angew. Chem., Int. Ed.* **2011**, *50* (11), 2532–2535.
(43) Calabrese, M. F.; Eakin, C. M.; Wang, J. M.; Miranker, A. D. *Nat. Struct. Mol. Biol.* **2008**, *15* (9), 965–971.
(44) Qian, J.; Noebels, J. L. *J. Physiol.* **2005**, *566* (Part3), 747–758.
(45) Frederickson, C. J.; Koh, J. Y.; Bush, A. I. *Nat. Rev. Neurosci.* **2005**, *6* (6), 449–462.
(46) Talmard, C.; Bouzan, A.; Faller, P. *Biochemistry* **2007**, *46*, 13658–13666.
(47) Tsvetkov, P. O.; Kulikova, A. A.; Golovin, A. V.; Tkachev, Y. V.; Archakov, A. I.; Kozin, S. A.; Makarov, A. A. *Biophys. J.* **2011**, *99* (10), L84–L86.
(48) Tougu, V.; Karafin, A.; Zovo, K.; Chung, R. S.; Howells, C.; West, A. K.; Palumaa, P. *J. Neurochem.* **2009**.
(49) Zirah, S.; Kozin, S. A.; Mazur, A. K.; Blond, A.; Cheminant, M.; Ségalas-Milazzo, I.; Debey, P.; Rebuffat, S. *J. Biol. Chem.* **2006**, *281* (4), 2151–2161.
(50) Mekmouche, Y.; Coppel, Y.; Hochgrafe, K.; Guilloreau, L.; Talmard, C.; Mazarguil, H.; Faller, P. *ChemBioChem* **2005**, *6* (9), 1663–1671.
(51) Brender, J. R.; Hartman, K.; Nanga, R. P.; Popovych, N.; de la Salud Bea, R.; Vivekanandan, S.; Marsh, E. N.; Ramamoorthy, A. *J. Am. Chem. Soc.* **2010**, *132* (26), 8973–8983.
(52) Walkup, G. K.; Imperiali, B. *J. Am. Chem. Soc.* **1997**, *119*, 3443–3450.
(53) Giachini, L.; Veronesi, G.; Francia, F.; Venturoli, G.; Boscherini, F. *J. Synchrotron Radiat.* **2010**, *17* (Part 1), 41–52.
(54) Giachini, L.; Francia, F.; Veronesi, G.; Lee, D. W.; Daldal, F.; Huang, L. S.; Berry, E. A.; Cocco, T.; Papa, S.; Boscherini, F.; Venturoli, G. *Biophys. J.* **2007**, *93* (8), 2934–2951.
(55) Kozin, S. A.; Mezentsev, Y. V.; Kulikova, A. A.; Indeykina, M. I.; Golovin, A. V.; Ivanov, A. S.; Tsvetkov, P. O.; Makarov, A. A. *Mol. Biosyst.* **2011**, *7* (4), 1053–1055.
(56) Bush, A. I. *Neurobiol. Aging* **2002**, *23* (6), 1031–1038.
(57) Schlief, M. L.; Craig, A. M.; Gitlin, J. D. *J. Neurosci.* **2005**, *25*, 239–246.
(58) Hartter, D. E.; Barnea, A. *Synapse* **1988**, *2*, 412–415.
(59) Tamano, H.; Takeda, A. *Metallomics* **2011**, *3* (7), 656–661.
(60) Innocenti, M.; Salvietti, E.; Guidotti, M.; Casini, A.; Bellandi, S.; Foresti, M. L.; Gabbiani, C.; Pozzi, A.; Zatta, P.; Messori, L. *J. Alzheimer's Dis.* **2010**, *19* (4), 1323–1329.
(61) Huang, X.; Atwood, C. S.; Moir, R. D.; Hartshorn, M. A.; Tanzi, R. E.; Bush, A. I. *J. Biol. Inorg. Chem.* **2004**, *9* (8), 954–960.
(62) House, E.; Collingwood, J.; Khan, A.; Korchazkina, O.; Berthon, G.; Exley, C. *J. Alzheimer's Dis.* **2004**, *6* (3), 291–301.
(63) Sarell, C. J.; Wilkinson, S. R.; Viles, J. H. *J. Biol. Chem.* **2010**, *285* (53), 41533–41540.
(64) Rozga, M.; Bal, W. *Chem. Res. Toxicol.* **2011**, *23* (2), 298–308.
(65) Meloni, G.; Vasak, M. *Free Radical Biol. Med. 50* (11), 1471–1479.
(66) Kozlowski, H.; Luczkowski, M.; Remelli, M. *Dalton Trans. 39* (28), 6371–6385.
(67) Alies, B.; Badei, B.; Faller, P.; Hureau, C. Reevaluation of Copper(I) Affinity for Amyloid-β Peptides by Competition with Ferrozine–an Unusual Copper(I) Indicator. *Chem. Eur. J.* DOI: 10.1002/chem.201102746.
(68) Cherny, R. A.; Legg, J. T.; McLean, C. A.; Fairlie, D. P.; Huang, X.; Atwood, C. S.; Beyreuther, K.; Tanzi, R. E.; Masters, C. L.; Bush, A. I. *J. Biol. Chem.* **1999**, *274* (33), 23223–23228.
(69) Durand, J.; Meloni, G.; Talmard, C.; Vasak, M.; Faller, P. *Metallomics* **2010**, *2* (11), 741–744.
(70) Ciuculescu, E.-D.; Mekmouche, Y.; Faller, P. *Chem.—Eur. J.* **2005**, *11* (3), 903–909.
(71) Sitaud, B.; Solari, P.-L.; Schlutig, S.; Hermange, H. *Suppl. Proc.: Mater. Process.d Energy Mater.* **2011**, *1*, 61.